



Contents lists available at ScienceDirect

Optik

journal homepage: [www.elsevier.com/locate/ijleo](http://www.elsevier.com/locate/ijleo)

Original research article

# Support structure and optical alignment technology of large-aperture secondary mirror measured by back transmission method



Funan Yu\*, Shuyan Xu

Changchun Institute of Optics, Fine Mechanics and Physics, Chinese Academy of Sciences, Changchun 130033, China

## ARTICLE INFO

## Keywords:

On-orbit Assembly Space Telescope  
Large-aperture secondary mirror  
Precise tilt adjustment  
Flexible structure  
Stability testing

## ABSTRACT

The diameter of secondary mirror measured by back transmission method in the on-orbit assembly space telescope validation prototype with a 1-meter aperture is  $\Phi 322$  mm, and the distance between secondary mirror and mounting surface is 2.5 m. The requirements for supporting structure are as follows: surface figure error caused by supporting structure should be better than 3.88 nm, the tilt stability of secondary mirror is better than 2", and the displacement error in the direction of optical axis is 0.04 mm. According to the above requirements, the supporting structure and alignment method of the secondary mirror are illustrated in detail, and the physical testing is completed. Firstly, the size parameters are optimized by the method of Orthogonal Optimization and Finite Element Analysis (FEA), based on the optimized result, the supporting structure is designed, the bonding mode of the mirror body, the flexible structure to release stress and the implementation method of 4-DOF precise adjustment are emphasized, the results simulated by FEA show that the optical axis displacement of the secondary mirror is 5.2  $\mu\text{m}$  and the error of the surface figure accuracy is 3 nm under the temperature range of 4°C and gravity load. Finally, the alignment process and steps without the primary mirror as the benchmark are described in detail. The stability of the supporting structure is tested, and the test period is 14 days. The results and practice indicate that surface figure accuracy is 0.01  $\lambda$  ( $\lambda = 632.8$  nm), structure remains stable to excellent levels that the tilt is 1" and the displacement is 0.02 mm under gravity and thermal loading, all of them meet the requirements of the optical system for the supporting structure, the design is reasonable, the effect is good.

## 1. Introduction

On-orbit Assembly Space Telescope is to modularize the telescope, send the segments into the predetermined orbit once or several times, and complete the telescope assembly on orbit. Validation prototype of telescope with a 1-meter aperture is developed for verification of related technologies, is shown in Fig. 1, the primary mirror is divided into six segments. With the help of single-axis turntable, the industrial robot integrated with hand-eye camera and pressure transducer assembles the primary mirror.

The optical diameter of secondary mirror in the on-orbit assembly space telescope validation prototype is  $\Phi 322$  mm, and the distance between secondary mirror and mounting surface is 2.5 m, for such a large-aperture and long span, the traditional support method is mainly backside support structure [1–6], however, back transmission method is adopted for the measurement of surface figure accuracy of secondary mirror in this system, so, it is not suitable to use the backside support structure for lightweight mirror body. Besides, optical alignment of the secondary mirror of traditional space telescope is based on the primary mirror [7–11],

\* Corresponding author.

E-mail address: [yufunan33@163.com](mailto:yufunan33@163.com) (F. Yu).<https://doi.org/10.1016/j.ijleo.2020.164274>

Received 9 December 2019; Accepted 19 January 2020

0030-4026/© 2020 Elsevier GmbH. All rights reserved.

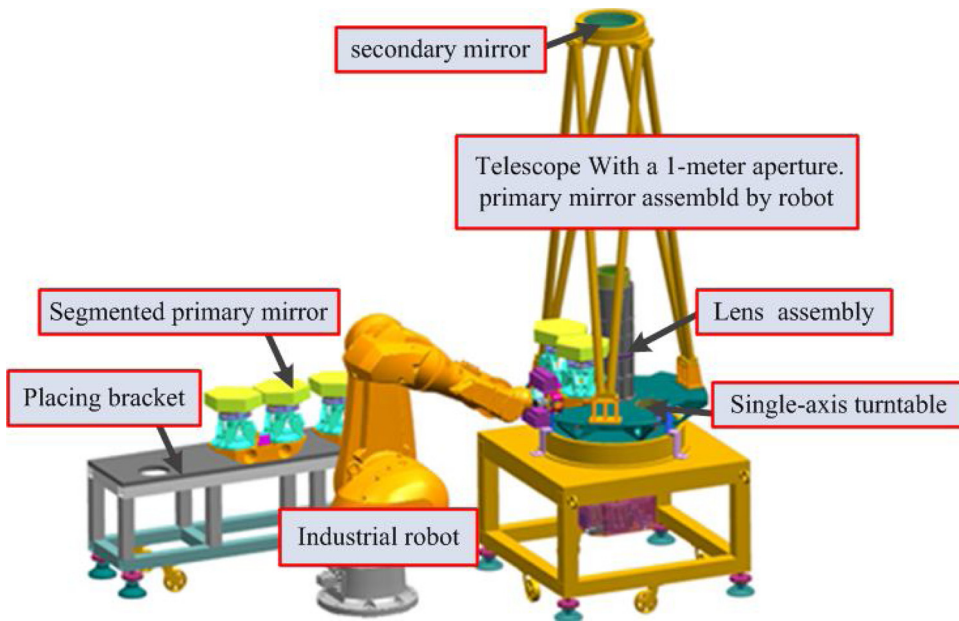


Fig. 1. On-orbit assembly space telescope validation prototype.

however, because the primary mirror of validation prototype is composed of segment arrays, it is the main object of assembly behavior, and it can't be used as the benchmark of the secondary mirror.

In view of the above two key problems about the secondary mirror, according to the relevant performance indicators of the optical system for the secondary mirror, this paper optimizes the design of the secondary mirror body, develops a new supporting structure for the large-aperture secondary mirror measured by back transmission method under the long span, explains the precise adjustment method of the secondary mirror, and verifies the supporting structure of the secondary mirror by FEA. without the primary mirror as the benchmark, a new alignment process and steps of the secondary mirror is designed. Finally, the stability of the secondary mirror supported by the designed structure is tested.

## 2. Design and analysis of support structure

### 2.1. Secondary mirror body

The optical diameter of secondary mirror is  $\Phi 322$  mm, measured by back transmission method, therefore, it is impossible to adopt the traditional axial backside support structure, and mirror body is not carried out by using method of light-weight design. In order to reach surface figure accuracy of the secondary mirror, the position of the supporting point should be far away from the mirror reflecting surface to avoid the influence of temperature load, assembly stresses and other factors. The structure of the secondary mirror body is shown in Fig. 2 below.

There are three working surfaces in the mirror body: optical reflecting surface, contact surface and adhesive surface. The size and position of the contact surface and the adhesive surface are the parameters to be optimized, as shown in Fig. 3, including the outer boundary dimension of the mirror  $\Phi A$ , the distance from the contact surface to the vertex of the reflecting surface is B, and the thickness of the center of the mirror body is C.

The orthogonal optimization method is adopted to determine the sizes of the mirror body [12], and the design level of each size

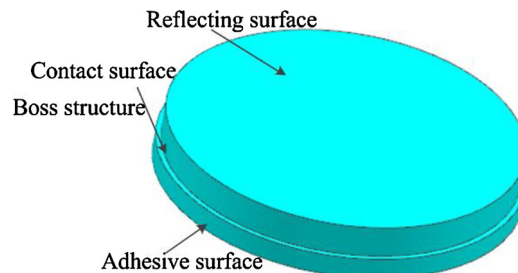


Fig. 2. Structural style of the secondary mirror body.

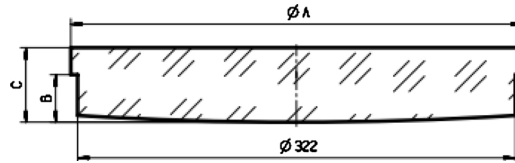


Fig. 3. Schematic diagram of optimized size of the mirror body.

parameter is shown in Table 1 below.

According to the factors of orthogonal test and level distribution, Select  $L_9(3^4)$  orthogonal table, and the simulation test arrangement is shown in Table 2.

The structural size of secondary mirror body is optimized under gravity and  $\pm 2^\circ\text{C}$  thermal load by FEA, taking surface figure accuracy as the evaluation target, and mesh generation of Hex-dominated with sweep, XSYMM boundary constraint is applied to the symmetrical plane whose normal direction is x, ZSYMM boundary constraint is applied to the symmetrical plane whose normal direction is z, and the contact surface is constrained by degree of freedom in Y direction to realize the full constraint of the mirror body. As the gluing between the mirror body and the mirror holder is completed in contact state, the degree of freedom of the adhesive surface is not constrained. The FEA model of the mirror body is shown in Fig. 4(a) and (b). After analysis and comparison, the final size parameters of the mirror body are determined as follows:  $\Phi A = 332\text{ mm}$ ,  $B = 35\text{ mm}$ ,  $C = 55\text{ mm}$ , the surface figure accuracy is better than  $1.45\text{ nm RMS}$ , which meets the optical requirements, and the deformation contour is shown in Fig. 4(c).

### 2.2. Support structure

The supporting structure of the secondary mirror should have high stability and large supporting stiffness. On the premise of meeting the above requirements, the influence on the figure accuracy of the secondary mirror should be as low as possible to meet optical requirements. The secondary mirror support structure is composed of support component of the secondary mirror body (SCSMB) and the support truss structure (STS). STS is the main body of long-span support, and it is also an important factor and guarantee to affect and maintain the stability of the system structure. SCSMB is directly connected with the mirror body, which should have good temperature adaptability and stress release function, so as to ensure that the figure accuracy of the secondary mirror is not degraded by the change of external load. SCSMB includes the secondary mirror body, the secondary mirror holder (SMH), the triangular support frame (TSF) and the adjusting components (AC). The mirror is made of quartz 7940, and SMH and TSF are made of invar 4J32, which has a lower coefficient of thermal expansion (CTE). The STS is composed of supporting rod and rod joint. The supporting rod is made of low CTE Carbon Fibre Reinforced Plastics (CFRP), and the rod joint is made of invar 4J32, as shown in Fig. 5 below. The mirror body is fixed on SMH by liquid glue. The TSF and the upper rod joint are connected by  $12 \times M6$  screws. The AC is used to adjust the secondary mirror precisely.

After the adjustment reaches requirements, the SMH is fastened on the TSF by  $6 \times M6$  screws.

The STS is constructed in the form of 6-bar mutually triangular structure. The triangle has high stability, which can ensure the strength and rigidity of the whole truss. This is a typical kinematic method, which can make the STS not generate internal stress to affect the stability of the structure due to over-constrained. At the same time, the truss in this structure form can also reduce the blocking of the incident ray and increase light energy.

In order to ensure the temperature adaptability and avoid the internal stress caused by the temperature change, the material of the SMH is 4J32 with identical CTE to mirror, as shown in Fig. 6 below. The flatness of the contact surface with the secondary mirror boss is  $0.002\text{ mm}$ , so as to ensure the contact area, improve the contact stiffness and no stress generation after glue curing. The width of the injection-glue groove is  $8\text{ mm}$ , and the depth is  $0.05\text{ mm}$ . The injection behavior is carried out through six evenly M3 thread holes.

The TSF is a transition part connecting the SMH and the STS, which has the function of balancing and releasing the stress caused by the mismatch of CTE between them. As shown in Fig. 7 below, the change of temperature will lead to the extension and contraction of the support rod. Because of a certain angle between the support rod and the vertical direction, the horizontal force component and the vertical force component will be formed and the bending stress will be generated between the TSF and the upper rod joint. The deformation will be produced when the TSF is squeezed, which is finally transmitted to the secondary mirror reflecting surface, and will affect the figure accuracy of the secondary mirror. Therefore, the release structure should be set to solve the above bending stress problem.

The TSF is shown in Fig. 8. There is a flexible set designed at the contact part with the upper rod joint. The coplanarity of the three

**Table 1**  
Design level table of size parameters unit: mm.

parameter	level1	level2	level3
$\Phi A$	$\Phi 327$	$\Phi 332$	$\Phi 337$
B	32	35	38
C	45	50	55

**Table 2**  
Orthogonal table of simulation analysis unit: mm.

line number	ΦA	B	C
1	Φ327	32	45
2	Φ327	35	50
3	Φ327	38	55
4	Φ332	32	50
5	Φ332	35	55
6	Φ332	38	45
7	Φ337	32	55
8	Φ337	35	45
9	Φ337	38	50

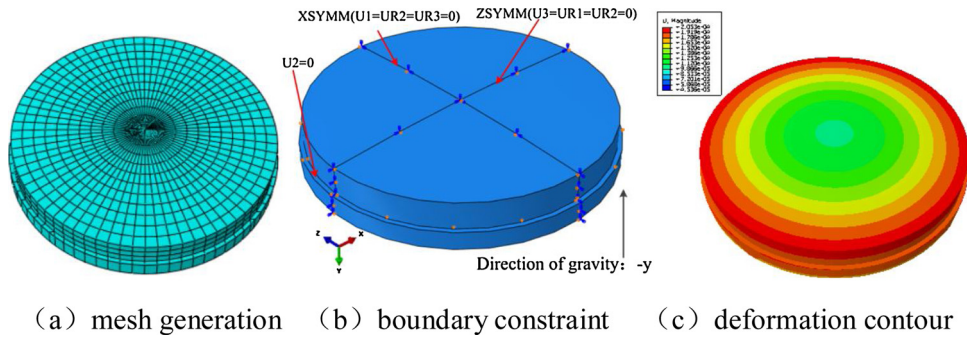


Fig. 4. Finite element model and analysis result.

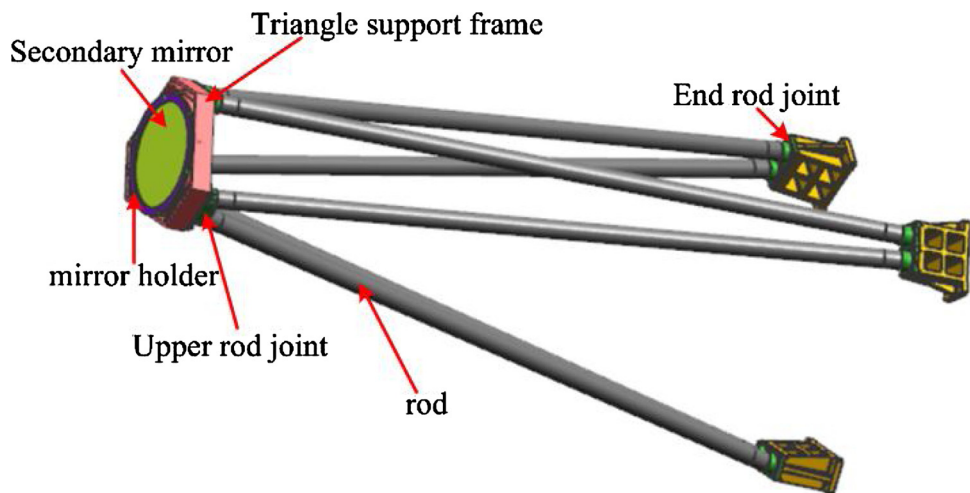


Fig. 5. Support structure.

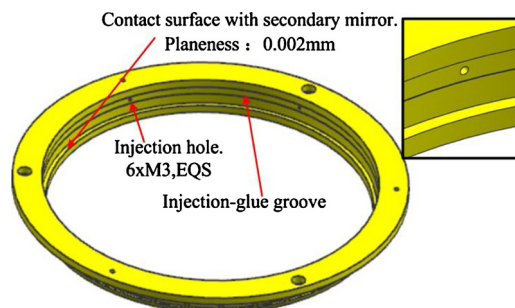


Fig. 6. SMH structure.

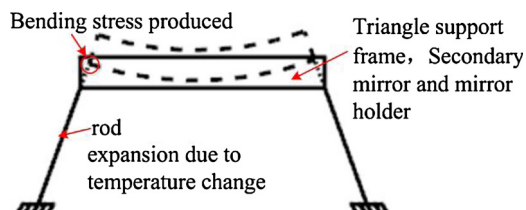


Fig. 7. Bending stress between TSF and STS.

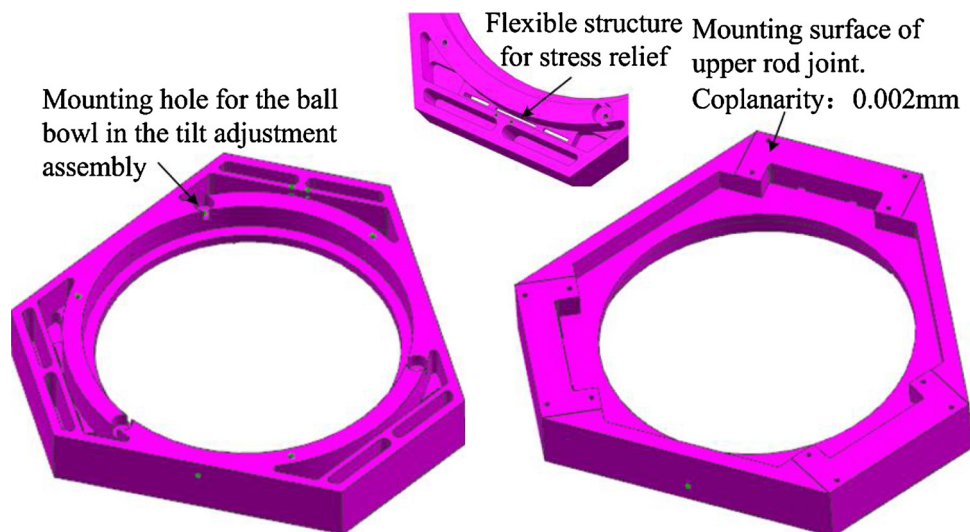


Fig. 8. TSF structure.

reference surfaces is 0.002 mm, six M6 thread holes are uniformly distributed on the contact surface with the SMH, which are used to fix the SMH, and three of which are in the assembly holes of the ball bowl in the tilt adjusting component.

### 2.3. Degree of freedom (DOF) adjustment component

In the optical system, the tilt stability of secondary mirror is better than 2" (the coaxiality error based on the correction lens assembly is 0.02 mm), and the displacement error in the direction of optical axis is 0.04 mm. Under such a long span, it is difficult to meet the above tolerance requirements through the processing of structural parts and the components assembly. Therefore, the high-precision DOF adjustment should be set to meet the optical index requirements. The adjustment method is shown in Fig. 9. The adjusted DOF includes two tilt DOFs and one translational DOF in the direction of optical axis.

Three groups of evenly tilt adjustment components are adopted to realize the precise adjustment of the tilt freedom of the secondary mirror, as shown in Fig. 9 above. The components include the upper ball bowl, the end ball bowl, the copper bush, the adjusting screw, and the M6 set screw, of which the upper ball bowl, the end ball bowl and the adjusting screw are made of 45# steel. The end ball bowl is assembled in the mounting hole of the TSF through the interference fit. The internal and external side of the copper bush are processed with threads, the copper bush is installed on the SMH through male thread, and the epoxy is added to fix, so as to prevent it from rotating when adjusting the tilt freedom of the secondary mirror, thus affecting the adjustment accuracy and stability after adjustment. Both ends of the adjusting screw are machined with spherical surface with a 20 mm radius. Aiming to realize the release the freedom of rotation, the upper spherical surface of the screw is matched with the spherical surface of the upper ball bowl, similarly, the end spherical surface of the screw is matched with the spherical surface of the end ball bowl. The male thread of the adjusting screw cooperates with the female thread of the copper bush to realize the precise adjustment of the angle, and the pitch of screw is 0.2 mm. In order to avoid interference between the male thread of M6 set screw and the inner surface of the adjusting screw during the adjustment process, there is a gap of 1 mm left between the two parts.

The aligning screw component produces a supplementary adjustment function of DOF of tilt, which is composed of M5 set screw and the push block. The push block is made of 2A12 aluminum alloy material, which is used for the homogenization of the applied force during the adjustment process to avoid too large concentrated stress effect which affects the figure accuracy of the secondary mirror on the SMH. The contact surface between the set screw and the push block is a sphere with a diameter of  $\Phi 30$  mm, the purpose of this is to release the rotational degrees of freedom to prevent it from producing over-positioning to the secondary mirror.

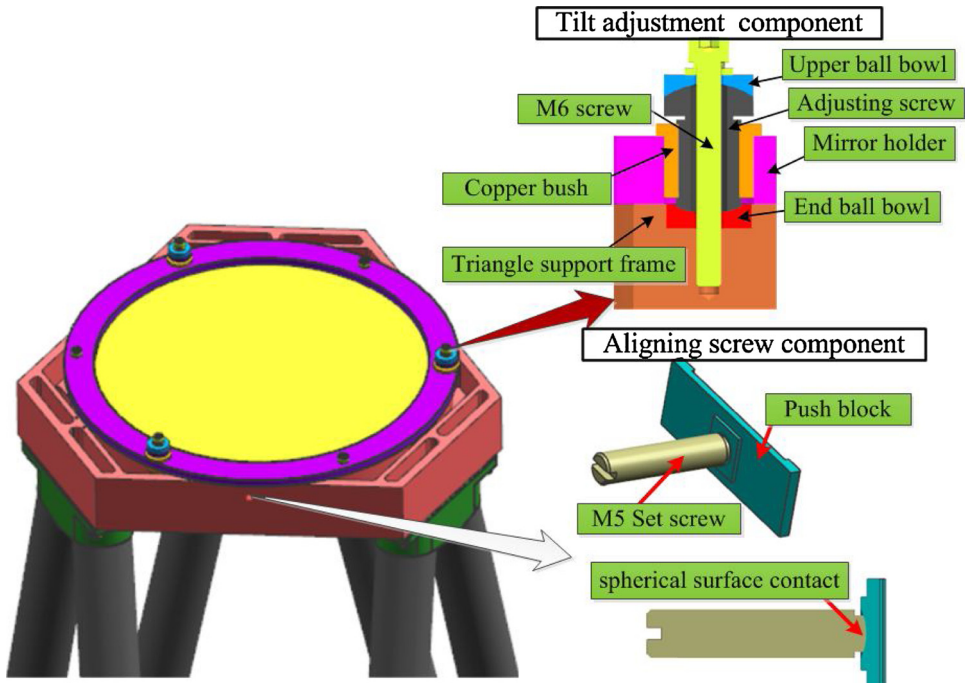


Fig. 9. DOF adjustment method.

2.4. FEA of structure

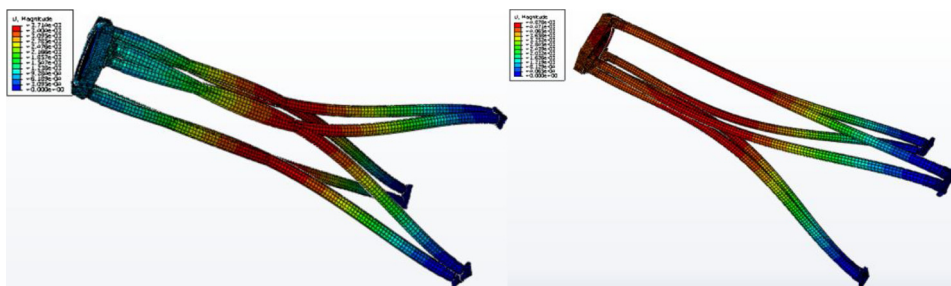
The overall supporting structure of the secondary mirror is analyzed by FEA, and the rationality of the above structure design is evaluated. Two working conditions are analyzed respectively: (1) combined action of gravity load and  $-2\text{ }^{\circ}\text{C}$  thermal load; (2) combined action of gravity load and  $+2\text{ }^{\circ}\text{C}$  thermal load. The analysis results is shown in Fig. 10 and Table 3.

The results show that under the temperature range of  $4\text{ }^{\circ}\text{C}$ , the displacement in the optical axis direction is  $5.2\text{ }\mu\text{m}$ , the off-centre and tilt are both zero, and the surface figure accuracy is  $3\text{ nm}$ , all of which meet the requirements of optical system. In the finite element simulation the off-centre and tilt are zero, which is not consistent with the actual situation. This is because the FEA is an ideal symmetrical model which is difficult to simulate the real situation of the internal residual stress of the structural parts, the assembly error, and the contact between parts.

3. Assembly and Test

The traditional secondary mirror alignment is based on the primary mirror, but for the segmented telescope system, the primary mirror can't be used as a benchmark. Therefore, the lens assembly is used as the alignment benchmark of the secondary mirror. The specific alignment method is as follows:

- (a) First, assemble a flat glass with crosshair on the front of the lens assembly, and use the Optical Alignment Instrument (OAI) to adjust the flat glass to ensure that the tilt error relative to the optical axis of the lens group is controlled within  $0.5''$ , and the off-



(a) condition1 deformation contour (b) condition2 deformation contour

Fig. 10. Deformation contour of support structure.

**Table 3**

Analysis results of surface figure accuracy.

condition	displacement(um)	off-centre (um)	Tilt(°)	RMS(nm)
1	0.6	-2.1476e-3	7.86e-4	3.06
2	-4.64	-1.4128e-3	9.8e-4	3.08

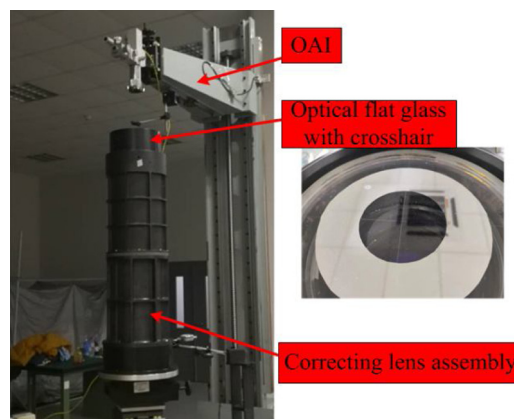
centre error between the crosshair and the optical axis of the lens group is controlled within 0.008 mm, as shown in Fig. 11.

- (b) Assemble the lens assembly integrated with flat glass on the single-axis turntable, and then assemble the rod in the STS, the truss should have a certain assembly position accuracy to adapt to the adjustment of secondary mirror's spatial position in the optical system. The clearance between the TSF and the SMH is 1 mm, that means that the maximum adjustment amount is 1 mm. Therefore, it should be ensured that the off-centre error between the central axis of the TSF and the flat glass crosshair is controlled within 1 mm. Because the TSF is a hollow structure and has no central positioning function, it is difficult to be used as the physical benchmark in the process of assembly and adjustment. In this regard, the fixture is used to replace the TSF and is processed with the same size of installation surface of the upper rod joint as the TSF. In order to leave a certain amount of redundancy for the adjustment of the tilt, the center is equipped with a  $\Phi$  0.2 mm positioning component for threading, as shown in Fig. 12.

Three upper rod joints are installed on the mounting surface of the fixture and so are positioned on a plane. The table of the single-axis turntable is leveled by the leveling device, and tested by the Electronical Gradienter. The threading hole on the fixture are adjusted to be coaxial with the flat glass crosshair by the plumb bob, as shown in Fig. 13, when reaching the good state, tighten the screws of the upper and end rod joints, and at the same time, observe whether the plumb bob moves, if it changes, readjust it, number the rod and its matching rod joints, and remove the rod joints on the fixture, by contrast, the end rod joints will not be removed, then J133 glue is used to bond the joint of rod and rod, and the coaxiality was rechecked by plumb bob to complete the assembly of rods.

- (c) After curing, then assemble the TSF, place the glued assembly which included the secondary mirror and the SMH (as shown in Fig. 14 for the surface figure accuracy test results) on the TSF for the installation and adjustment of the secondary mirror, and the process is carried out on the air-floating platform to eliminate the impact of external vibration on the installation and adjustment. The specific process is as follows: firstly, the flat glass is calibrated by Leica TM6100A and high-precision plane reflecting mirror which are placed on the 4-meter high bracket, concentric calibration is completed by near-field image, and tilt calibration is completed by far-field image, then, place the glued assembly on the TSF for precise adjustment. During the adjustment process, ensure that the Leica and the plane reflecting mirror are not affected by the external interference force and the position has no changes, as shown in Fig. 14.
- (d) Monitor the stability of the secondary mirror for 14 days. After the secondary mirror is installed and adjusted, keep the position of Leica, plane reflecting mirror and secondary mirror free from human or external load disturbance, considering the lack of Y-direction rigidity of the 4-meter high bracket, after 7 days of monitoring, the electric driven single-axis turntable rotates  $90^\circ$ , and the secondary mirror is calibrated again, and then monitored for other 7 days, so as to eliminate the deformation error caused by the lack of Y-direction stiffness of the 4-meter high bracket. The monitoring results are shown in Fig. 15 below, and the test results show that the stability meets the requirements of 2 ".

The spatial distance stability of the secondary mirror relative to the lens assembly is monitored by a three coordinate measuring arm. The measurement process is shown in Fig. 16. the measurement results show that the stability of the secondary mirror in the optical axis direction is 0.02 mm, meeting the stability requirement of 0.04 mm.

**Fig. 11.** Flat glass assembly.

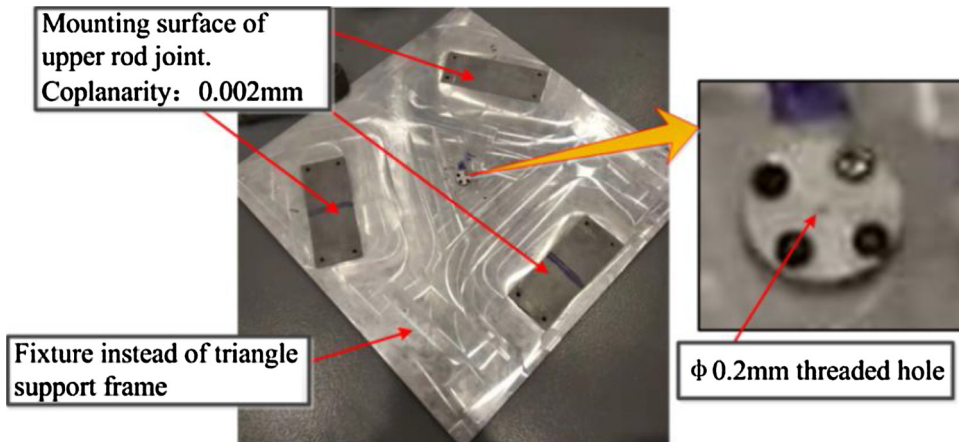


Fig. 12. Fixture for alignment.

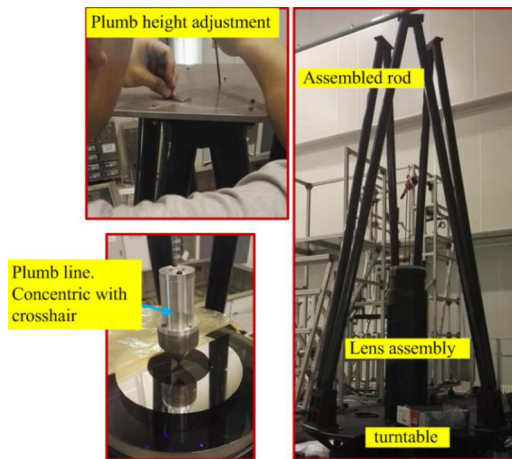


Fig. 13. Assembly of rods.



Fig. 14. Precise adjustment of secondary mirror.

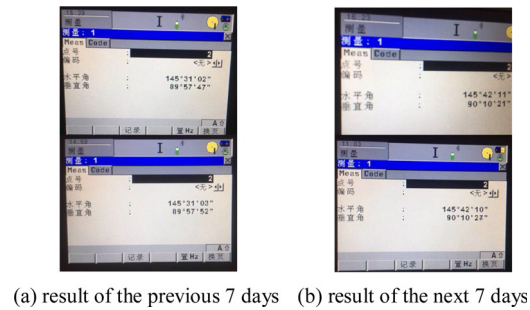


Fig. 15. Tilt stability test results.

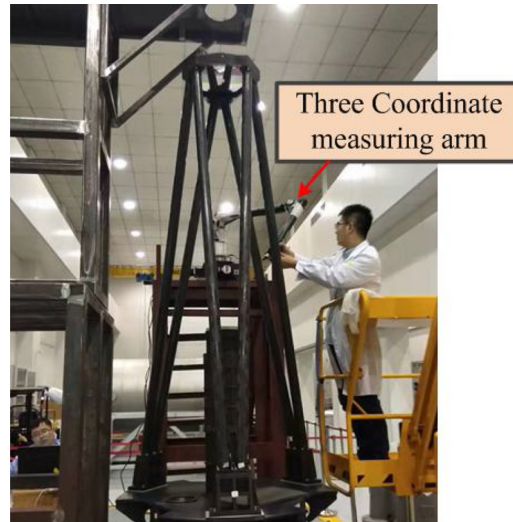


Fig. 16. Stability test in optical axis direction.

#### 4. Conclusion

This paper introduces a new kind of supporting structure and its installation and adjustment method applied to the large-aperture secondary mirror. It focuses on the optimization design of the size parameters of the mirror body, also on the research on the implementation method of the secondary mirror holder, flexible structure setting of triangular support frame and DOF adjustment components in the supporting structure. The alignment process and steps without the primary mirror as the benchmark are described. The results show that the surface figure accuracy is  $0.01\lambda$ , the stability is  $1''$  and  $0.02$  mm, all of which meet the requirements.

#### Acknowledgements

This research was supported by the program of Research on Key Technology of Ultra Large-aperture On-Orbit Assembly Space Telescope (The program number is 2016YFE0205000), which comes from Ministry of Science and Technology of the People's Republic of China.

#### References

- [1] X. Hongwei, Y. Jinsong, G. Minghui, et al., Support design for secondary mirror of high resolution space telescope, *Infrared Laser Eng.* 40 (9) (2011) 1724–1729.
- [2] Y. Yue, L. Wei, Design and analysis for secondary mirror of space remote sensor by parameterization method, *J. Appl. Opt.* 36 (6) (2015) 836–840.
- [3] P.R. Yoder, *Opto-Mechanical System Design*, Cooperate Marcel Dekker Inc, US, 1993.
- [4] P. Schipani, F. Perrotta, C. Molfese, et al., The VST secondary mirror support system, *SPIE Astronomical Telescopes + Instrumentation. International Society for Optics and Photonics* (2008) 701845-701845-10.
- [5] L. Xiaoming, *Optimization Design of Space Large Aperture Telescope Optical Machine Structure*, Shanghai Institute Of Technical Physics, Chinese Academy Of Sciences, Shanghai, 2018.
- [6] D.R. Neill, W.J. Gressler, J. Sebag, LSST secondary mirror assembly baseline design *SPIE, Ground-Based and Airborne Telescopes IV*, (2012) 84440J-84440J-19.
- [7] S. Kim, S. YANG H, W. LEE Y, et al., Merit function regression method for efficient alignment control of two-mirror optical system, *Opt. Express* 15 (8) (2007) 5059–5068.
- [8] H. LEE, G.B. DALTON, I. TOSH, Computer-guided alignmentII:optical system alignment using differential wavefront sampling, *Opt. Express* 15 (23) (2007) 15424–15437.

- [9] G. Xu, S.H.M. Yang, Y.B. Gong, Optimal design of pose and position fine tuning apparatus for secondary mirror in large optical telescope, *Opt. Precis. Eng* 16 (7) (2008) 1181–1189.
- [10] W. Bin, J. Shilei, Study on computer-aided alignment method of cassegrain system, *Opt. Inst.* 2 (30) (2008) 50–54.
- [11] Z. Xiangming, J. Feng, K. Longyang, et al., Research on optical alignment technology for Cassegrain system, *J. Appl. Opt.* 36 (4) (2015) 526–530.
- [12] Y. Funan, Research of the Double Bending Vibration Modal Transformation Piezoelectric Motor, Harbin Institute Of Technology, Harbin, 2012.